

# Electrochemical Performance and Functionalization of Multiwalled Carbon Nanotubes with a Green and Facile Treatment

L.L. Guo<sup>1</sup>, Z.H. Luo<sup>1,\*</sup>, Y.Z. Zhao<sup>1</sup>, J. Guo<sup>1</sup>, M. Zhu<sup>1</sup>, K. Luo<sup>1,†</sup>, A.Z. Huang<sup>2</sup>

<sup>1</sup>Guangxi Key Laboratory of Universities for Clean Metallurgy Comprehensive Utilization of Nonferrous Metal Resource, Guilin University of Technology, Guilin, 541004, PR China

<sup>2</sup>Humanwell Healthcare (GROUP)CO., LTD, Wuhan, 430075, PR China

Received: December 28, 2017, Accepted: October 15, 2018, Available online: March 28, 2019

**Abstract:** Functionalization of multiwalled carbon nanotubes (MWNTs) are proceeded with cold plasma generated in N<sub>2</sub> and air atmosphere. X-ray photoelectron spectroscopy (XPS) shows that the nitrogen and/or oxygen elements are incorporated into MWNTs. The total nitrogen contents are approximately equal in N<sub>2</sub> and air atmospheres, while oxygen content is increased significantly in air atmosphere, the species and content of the functional groups depend on the applied gases. Transmission electron microscope (TEM) shows that the morphology of functionalized MWNTs is almost the same to pristine MWNTs, although functional groups and defects increase. The electrochemical experiments results demonstrate that introduction of functional groups enhance the pseudocapacitance, while the cyclic stability of the functionalized MWNTs is as well as the pristine MWNTs.

**Keywords:** Cold plasma, Multiwalled carbon nanotubes, Functionalization, Supercapacitor

## 1. INTRODUCTION

Carbon nanotubes (CNTs) have attracted tremendous attentions for their outstanding mechanical properties, conductivity, huge specific surface area and chemical stability, [1] which have been used in various fields, such as electronic device, batteries, supercapacitors, and et al. However, the inert surface properties of pristine CNTs limits their applications due to the weak interaction with other materials and poor wettability. Nowadays, functionalization such as heteroatom doping, surfactant or polymer modification is applied to improve the above mentioned properties. Surfactant (or polymer) and CNTs are combined by covalent bond without destroying intrinsic character of CNTs [2-3], however, the conductivity of modified CNTs is decreased due to the insulated surfactant and polymer, thus this kind of modified CNTs is not suitable for the circumstances which require high conductivity, such as the field of batteries, supercapacitors and other energy storage devices.

Heteroatom doping is widely applied to functionalize carbon nanotubes, even other carbon materials, such as, graphene, carbon nanofibers. The heteroatoms, for example, N, O, B, S and P can improve the conductivity and wettability. [4-7] Among which, N doping is widely used because nitrogen groups can significantly enhance the performance of supercapacitors and batteries, even nitrogen doped carbon materials can be used as metal-free electrocatalysts for oxygen reduction reactions. [8] Previous studies demonstrated that nitrogen doped carbon materials can be prepared with the following methods: (1) graphitizing nitrogen contained precursor via chemical vapor depositing, direct current magnetron

sputtering and etc; [9-10] (2) carbonizing nitrogen-rich polymer or precursors; [11-12] (3) post treating the carbon materials in the nitrogenous atmosphere, such as N<sub>2</sub> or NH<sub>3</sub> and etc. [13-14]

By using the first methods, nitrogen exists in the internal and external wall of CNTs resulting in high nitrogen content and wall torsion. Suenaga and co-workers found that the nitrogen content was in the range from 13 at.% to 30 at.% by adjusting the ratio of N<sub>2</sub>/Ar with direct current magnetron sputtering. [9] Liu and co-workers' reported that the morphology transformed from straight and smooth walls to cone-stacked shape or bamboo-like structure with increasing of nitrogen content by using a floating catalyst chemical vapor deposition method. [10] However, the device is complicated and expensive. Compared to the first methods, the preparation of N-CNTs with the second methods is facile to realize, but careful control of raw materials' morphology and carbonization condition are needed to form the tubular structure. With the application of the third methods, heat, plasma or N<sub>2</sub><sup>+</sup> ion beam, ball milling and etc are employed to prepare N-CNTs with the improved property while the original morphology and structure of CNTs is almost unchanged. During which, plasma or N<sub>2</sub><sup>+</sup> ion beam treatment is an environment-friendly, time-saving method to functionalize CNTs, however vacuum environmental is required, and the structure of CNTs is destroyed when the high energy beam is applied, [13] more milder methods are needed to explore.

It is reported that cold plasma treatment is used to functionalize materials in ambient temperature and pressure with low destruction. [15-17] In this paper, N<sub>2</sub> and/or air-generated cold plasma are adopted to functionalize MWNTs by using home-made plasma generator without high temperature and vacuum, the time required for nitrogen doping is short and no post treatment processes are

To whom correspondence should be addressed: Email: luozhihong615@glut.edu.cn (\*), Email: luokun@glut.edu.cn (†)

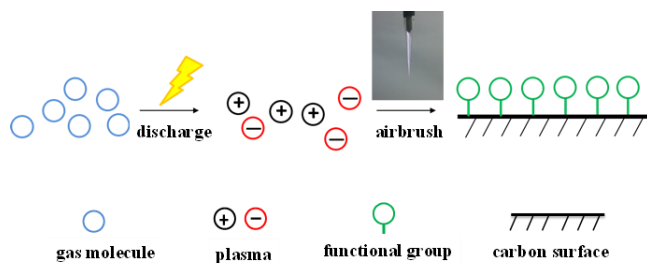


Figure 1. Illustration for functionalization of MWNTs by cold plasma treatment.

needed. The content and species of nitrogen groups, as well as oxygen groups induced by  $N_2$  and/or air are investigated comparatively, where the total nitrogen content is about 0.9 at.%, oxygen content increased about 2.4 at.% in air, the species of functional groups are varied with the applied gases. The electrochemical behavior and the effect of functional groups on the performance of functionalized MWNTs are studied in detail, by incorporation of functional groups, the specific capacitance is increased while the cyclic stability is maintained.

## 2. EXPERIMENTS

### 2.1. Materials

Raw multi-walled carbon nanotubes with 5-15  $\mu\text{m}$  in length and 20-50 nm in diameter were purchased from Shenzhen Nanotech Porch Co., Ltd., China.  $N_2$  with the purity of 99.9% and air pumped from atmosphere were used to generate plasma.

### 2.2. Cold plasma treatment of MWNTs

The home-made cold plasma device was used to functionalize MWNTs with corona discharge mode. A plasma generator was connected to a discharge chamber with two nickel electrodes wrapped on its outer wall. The cold plasma can be generated when the gas passed through the chamber and the voltage was applied between the two electrodes. In this paper, the gas was partly excited by using alternating current (AC) with a voltage amplitude value of 50 V and a power of 21 W. Before power on, the remained gas in the container was removed flowing gas for 30 min. The plasma flowed with the gas through a bush to blow from the bottom of

container where pristine MWNTs were placed and to functionalize MWNTs. All the cold plasma treatment process lasted 30 min during which the process was paused to cool down the device in every 2 min. The samples treated by the  $N_2$  and air-generated cold plasma were named as MWNT-N and MWNT-A, respectively.

### 2.3. Characterization

The element composition of the samples was measured on X-ray photoelectron spectroscopic instrument (XPS, ESCALAB250Xi, Thermo). Raman spectra were obtained on a Thermo Fisher DXR Raman spectrometer equipped with a 532 nm incident laser light source. The morphology images were obtained on Field emission transmitting electron microscopy (TEM, JEOL, JEM-2100F) in low vacuum mode. XRD spectra were recorded on X-ray diffractometer (XRD, X'Pert PRO).

### 2.4. Electrochemical measurements

All electrochemical measurements were performed in a three-electrode setup. Pt foil and saturated calomel electrode (SCE) was used as counter and reference electrode, respectively, and 6 mol  $L^{-1}$  KOH was used as electrolyte. The working electrode was prepared by mixing 20  $\mu\text{L}$  of ethanol, 10 mg of as-prepared samples, 10  $\mu\text{L}$  of 5% poly(tetrafluoroethylene) (PTFE) to obtain slurry which was pressed on the nickel foam substrates (1 cm  $\times$  1 cm) and dried at 60  $^{\circ}\text{C}$  for 5 h.

## 3. RESULTS AND DISCUSSION

$N_2$  and air generated cold plasma are used to modify the surface of multi-wall carbon nanotubes, respectively. As the illustration showed in Fig.1, air (mainly includes  $N_2$  and  $O_2$ ) or  $N_2$  is ionized to form plasma during the discharge process. The cold plasma sprays through the airbrush and acted on MWNTs to create functional groups on the surface or subsurface of carbon. The illustration is showed in Fig.1. The flame image is Ar plasma because its blue flame is obvious to observe.

The structure of functionalized MWNTs is measured by Raman and XRD analysis. Raman spectra (Fig.2a) of MWNT-N, MWNT-A and pristine MWNTs exhibit two prominent peaks corresponding to the disordered (D) band and graphitic (G) band, respectively. D band is attributed to a breathing mode of  $K$ -point phonons of  $A_{1g}$  symmetry, which is related to the defects in graphitic structure. G band arises from an  $E_{2g}$  mode which related to the vibration in all  $sp^2$ -bonded carbon atoms. [18] The high intensity of D band of

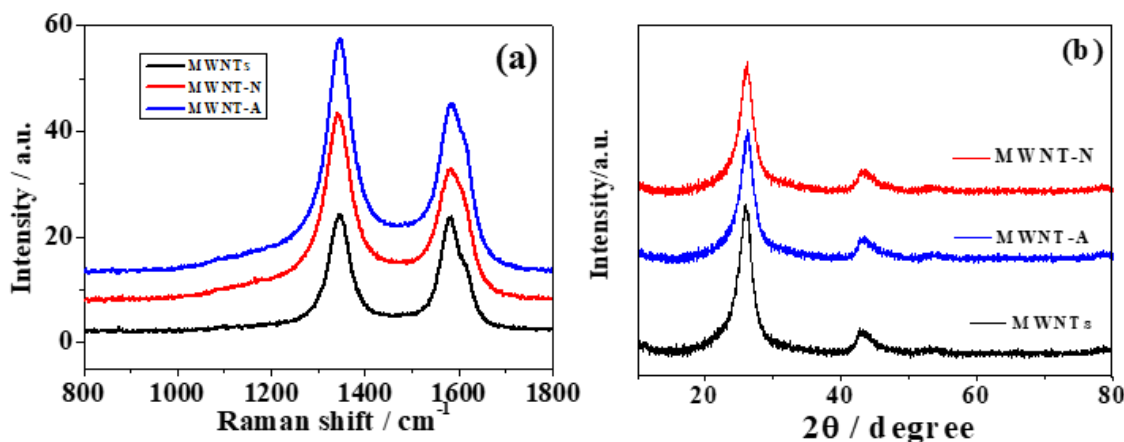


Figure 2. Raman (a) and XRD pattern (b) of MWNTs, MWNT-N and MWNT-A.

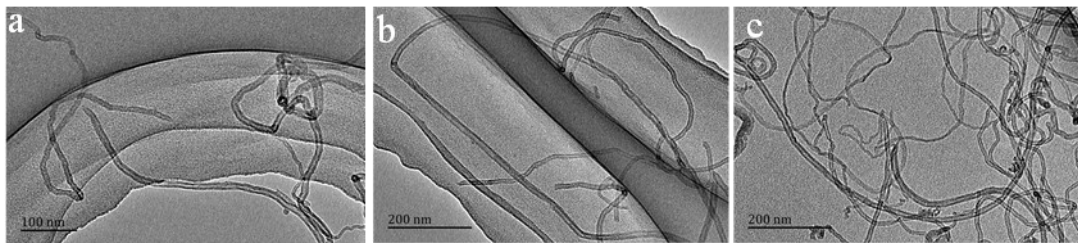


Figure 3. TEM images of MWNTs(a), MWNT-N(b) and MWNT-A(c)

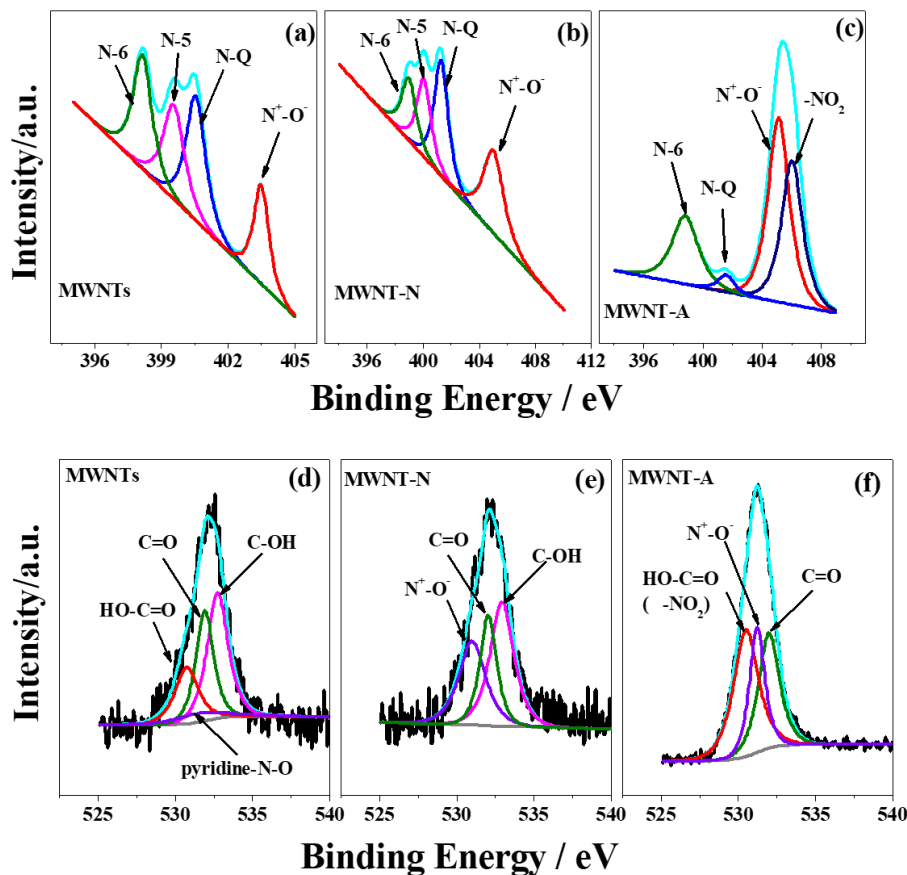


Figure 4. N1s (a, b, c) and O1s (d, e, f) spectra of MWNTs (a, d), MWNT-N(b, e) and MWNT-A(c, f).

MWNTs is due to the post acid-treatment for removing metal catalyst. The  $I_D/I_G$  ratio of MWNTs (about 1) increases to 1.35 and 1.34 after  $N_2$  and air cold plasma treatments, respectively. The increased  $I_D/I_G$  ratio demonstrates the increased defects of MWNTs because of the formation of functional groups. The XRD pattern is used to characterize the structure of nitrogen doped MWNTs. Two characteristic peaks located at around  $25.6^\circ$  and  $42^\circ$  correspond to the (002) and (100) planes of hexagonal carbon. [19]

TEM images (Fig. 3) show the morphology of MWNTs, MWNT-N and MWNT-A, all the samples exhibit a smooth, long and tortuous morphology, which is similar to pristine MWNTs. No notch and distortion are observed, the open ends of the carbon nanotubes are the position where the metal catalysts are removed by acid treatment before delivery. The unbroken tubes of MWNT-N and MWNT-A implies that the cold plasma act on the surface

and/or subsurface of MWNTs without serious damaging the structure, which elucidate that cold plasma treatment is a low destructive method for functionalization.

The distribution of surface nitrogen, oxygen functionalities of MWNTs, MWNT-N and MWNT-A are measured by the deconvolution of corresponding N1s and O1s high-resolution XPS signals, which are illustrated in Fig.4, Table 1 and Table 2. As showed in Table 1, the N and O species of pristine MWNTs are probable from the impurity in synthesis and post acid-treatment process. Nitrogen element is incorporated into MWNTs by  $N_2$  and air cold plasma treatment effectively, with the N atom percentage increasing from 0.39 at.% (MWNTs) to 0.9 at.% (MWNT-N) and 0.94 at.% (MWNT-A), respectively. Moreover, the oxygen content of MWNT-A is increased about 2.4 at.%, for MWNT-N, the oxygen content (1.02 at.%) is almost equal to MWNTs (1.03 at.%).

Table 1. C, O, N element content of MWNTs, MWNT-N, MWNT-A.

Species	At. %		
	MWNTs	MWNT-N	MWNT-A
C1s	96.83	96.07	90.19
O1s	1.03	1.02	3.47
N1s	0.39	0.9	0.94

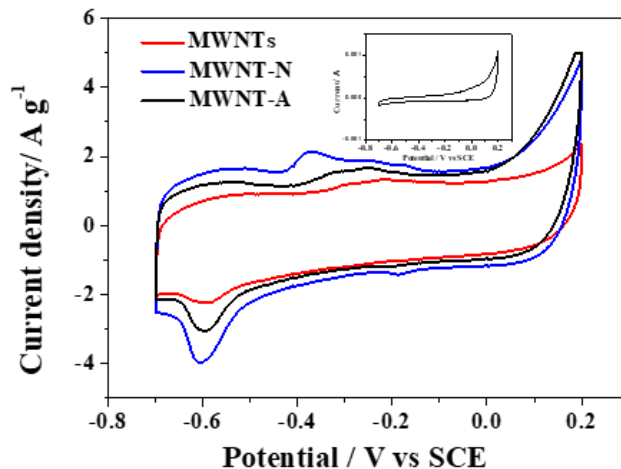
Table 2. nitrogen and oxygen species content of MWNTs, MWNT-N, MWNT-A

Species	At. %			
	MWNTs	MWNT-N	MWNT-A	
N	N-6	0.1	0.15	0.19
	N-5	0.09	0.19	N/A
	N-Q	0.12	0.28	0.03
	N <sup>+</sup> -O <sup>-</sup>	0.07	0.29	0.41
	-NO <sub>2</sub>	N/A	N/A	0.31
O	HO-C=O	0.25	N/A	0.84
	N <sup>+</sup> -O <sup>-</sup>	0.06	0.33	0.89
	C=O	0.31	0.27	2.67
	C-OH	0.41	0.43	N/A
	-NO <sub>2</sub>	N/A	N/A	0.62

The chemical states of nitrogen atoms with binding energies about 398.7 eV, 399.5 eV, 401.4 eV, 405.0 eV and 406.1 eV are identified as pyridine (N-6), pyrrole (N-5), quaternary nitrogen (N-Q) and pyridine-N-Oxide (N<sup>+</sup>-O<sup>-</sup>) and -NO<sub>2</sub>, respectively. [20] As Fig. 4a-c and Table 2 shows, nitrogen species of pristine MWNTs are mainly N-6, N-5, N-Q and a small amount of N<sup>+</sup>-O<sup>-</sup>. As for MWNT-N, the content of N-6, N-5, N-Q and N<sup>+</sup>-O<sup>-</sup> increase, the oxygen in N<sup>+</sup>-O<sup>-</sup> group possibly originates from the impurity of N<sub>2</sub> gas. As for MWNT-A, the content of N-6 increases compared to pristine MWNTs, while N-5 disappears possibly because N-5 is unstable in the oxidized atmosphere, [22] and oxygen-contained nitrogen species, such as N<sup>+</sup>-O<sup>-</sup> (0.41 at.%) and -NO<sub>2</sub> (0.31 at.%) increase significantly.

As for oxygen groups, the peaks at about 532.9 eV, 532.0 eV, 531.2 eV and 530.5 eV are attributed to C-OH, C=O, pyridine-N-oxide (N<sup>+</sup>-O<sup>-</sup>), and HO-C=O (-NO<sub>2</sub>), respectively. [21] It is worth noting that the -COOH group disappears in MWNT-N, the content of pyridine-N-oxide increases, the C-OH and C=O is almost identical to pristine MWNTs, which results in the oxygen content unchanged. While for MWNT-A, the C-OH groups vanished, -COOH and C=O groups increase significantly. The content of -NO<sub>2</sub> and -COOH groups is calculated to be 0.84 at.% and 0.62 at.% (the content of -COOH is calculated by subtracting doubled value of -NO<sub>2</sub> (at 406.1 eV) from the total content obtained from peak at 530.5 eV). These results demonstrate that the functional groups introduced into MWNTs depend on the applied gases.

The effect of functional groups on the electrochemical properties is estimated by using cyclic voltammetry (CV), galvanostatic charge-discharge and electrochemical impedance spectroscopy (EIS). Fig. 5 shows the CV curves of carbon nanotubes in 6 M

Figure 5. CV curves of MWNTs, MWNT-N and MWNT-A at 25 mV s<sup>-1</sup>, inset: CV curve of bare nickel foam.

KOH. It shows that all samples display a couple of redox peaks although which are not obvious in pristine carbon nanotube. The redox peaks are mainly originated from faradic current caused by the existence of active nitrogen and/or oxygen groups, because the redox peaks still preserve in the Ar saturated electrolyte (which is not showed here) and no redox peaks are observed on bare nickel foam (inset of Fig.5). The MWNT-N exhibits the highest reduction current density, followed by MWNT-A and MWNTs.

The galvanostatic charge-discharge curves are showed in Fig.6a and 6b. Due to the existence of faradic current, the charge-discharge curves deviated from linearity, especially for MWNT-N and MWNT-A at low current density. At high current density, the deviation is alleviated demonstrating the main contribution of EDLC at rapid charge-discharge process.

The specific capacitance is calculated from charge-discharge curves from the equation:

$$C = \frac{I\Delta t}{mV} \quad (1)$$

Where C is the specific capacitance (F g<sup>-1</sup>), I is the charge-discharge current (A), Δt is the discharge time (s), m is the mass of electrode materials (g), V is the potential window (ΔV).

The specific capacitances of MWNTs, MWNT-A and MWNT-N are showed in Fig.6c. The highest specific capacitance of 87 Fg<sup>-1</sup> is obtained from MWNT-N. At the current density of 0.2 Ag<sup>-1</sup>, 0.5 Ag<sup>-1</sup>, 1.0 Ag<sup>-1</sup>, 2.0 Ag<sup>-1</sup>, the specific capacitance of MWNT-N is 87 Fg<sup>-1</sup>, 59 Fg<sup>-1</sup>, 44 Fg<sup>-1</sup>, 40 Fg<sup>-1</sup>, respectively, which increases 40% more than that of MWNTs, especially at the current density of 0.2 Ag<sup>-1</sup>, the capacitance increases by 52.6% demonstrating significant contribution of pseudocapacitance. MWNT-N exhibits the highest capacitance at each current density, followed by MWNT-A and MWNTs. Fig.6d shows the cyclic stability of MWNTs, MWNT-N and MWNT-A, in which the capacitance retention decrease fast at the first 30 cycles, possibly due to the fast decay of the pseudocapacitance, after then these three samples can keep stable at least 4000 cycles with the capacitance retention about 79.3%, 82.5% and 79.5% for MWNTs, MWNT-N and MWNT-A, respectively.

According to the previous reports, N-5, N-6, C=O and C-OH contribute to the pseudocapacitance, [23] N-6 and N-Q improved the conductivity of carbon materials. [24] The total content of N-5,

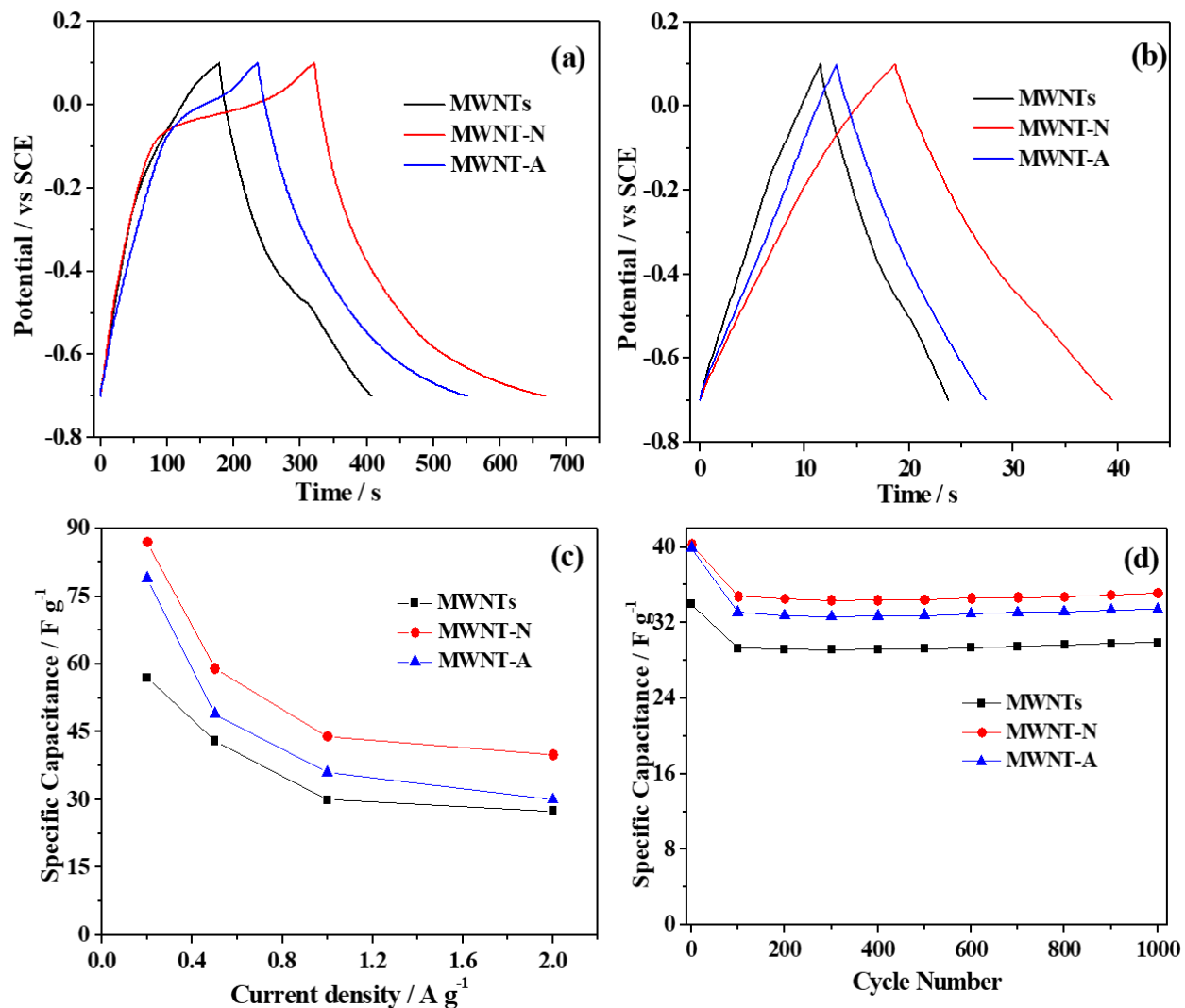


Figure 6. Charge-discharge curves of MWNTs, MWNT-N and MWNT-A at the current density of 0.2 Ag<sup>-1</sup>(a) and 2 Ag<sup>-1</sup>(b). Specific capacitance (c) and cycling stability (d) of MWNTs, MWNT-N and MWNT-A.

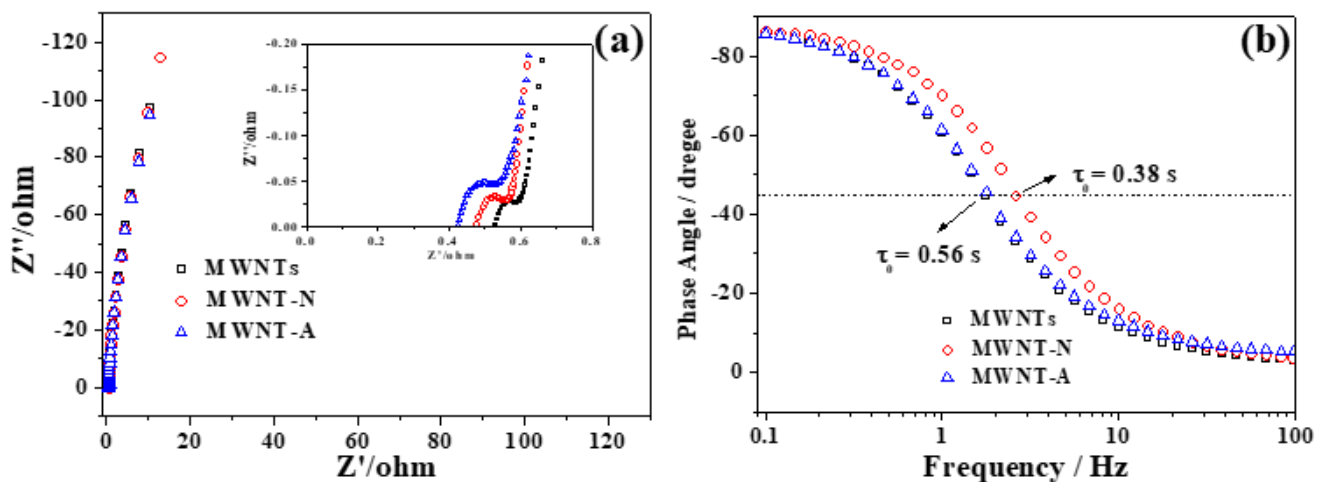


Figure 7. Nyquist plots (Fig.7a, inset: Nyquist plots at high frequency) and Bode plots (Fig.7b) of MWNTs, MWNT-N and MWNT-A.

N-6, N-Q, C=O and C-OH groups of MWNT-N are higher than those of MWNTs and MWNT-A, leading to higher pseudocapacitance. As for MWNT-A, the high content of C=O and N-6 improve their pseudocapacitance, however, compared to MWNT-N, the sum of N-6 and N-Q is lower, and the total content of N<sup>+</sup>-O<sup>-</sup>, -NO<sub>2</sub> and -COOH is higher, which could hinder the enhancement of supercapacitor performance.

To further understand their capacitive behaviors, the Nyquist plots of MWNTs, MWNT-N and MWNT-A are showed in Fig.7a, where the frequency ranges from 100 kHz to 0.01 Hz. All the Nyquist plots contain two parts: a semicircle and a straight line. As showed in the inset of Fig.7a, the intercept of horizontal axis which represents the equivalent series resistance (ESR) is reduced, possibly due to improvement of the wettability and conductivity caused by nitrogen and oxygen groups. [25] The small uncompleted semicircle of each plot at high frequency demonstrates low charge transfer resistance, which indicates the high conductivity of nitrogen doped carbon nanotubes. The characteristic frequency  $f_0$  at the phase angle of -45° is 2.61 Hz for MWNT-N and 1.78 Hz for MWNTs and MWNT-A, corresponding to the time constant  $\tau_0$  ( $\tau_0=1/f_0$ ) of 0.38 s and 0.56 s, respectively, the shorter time constant of MWNT-N indicates the faster charge-discharge rate compared to MWNT and MWNT-A. [26]

Based on the results, we consider that cold plasma is a green and facile method to modify carbon materials, where only functionalities and no other agents who influence the purity of carbon materials are introduced. Although the electrochemical performance is improved because of functionalization, the nitrogen groups content and specific capacitance of functionalized MWNTs are needed to enhance in future work.

#### 4. CONCLUSION

Nitrogen and oxygen groups are introduced to MWNTs with cold plasma treatment successfully. The content of introduced nitrogen is almost the same by using N<sub>2</sub> and air, however, the species of functional groups are different, the oxygen is introduced with considerable high content by using air. The morphology of pristine carbon nanotubes is preserved, while the disorder and defects are increased. The specific capacitance is increased for MWNT-N and MWNT-A, and the cyclic stability is maintained. We consider that the cold plasma treatment is a mild and effective method to functionalize the carbon materials without destroying the structure seriously, which also can be used for other carbon materials, such as graphene, carbon nanofibers and etc.

#### 5. ACKNOWLEDGEMENTS

This work was supported by Guangxi Natural Science Foundation (No. 2016GXNSFAA380107 and 2018GXNSFAA281184) and the funding from Key Lab of New Processing Technology for Nonferrous Metals & Materials Ministry of Education and Featured Materials and Collaborative Innovation Center for Exploration of Hidden Nonferrous Metal Deposits and Development of New Materials in Guangxi.

#### REFERENCE

[1] Z.B. Yang, J.Ren, Z.T. Zhang, et al., Chem. Rev., (2015),115, pp. 5159-5223.  
 [2] T.Morishita, M. Matsushita, Y.Katagiri, et al., Carbon, (2010),48, pp. 2308-2316.  
 [3] L. Mao, K. Zhang, H.S.O. Chan,et al., J. Mater. Chem., (2012), 22, pp. 80-85.

[4] J. Liang, Y. Jiao, M. Jaroniec,et al., Angew. Chem., (2012), 124, pp.11664-11668.  
 [5] Z.B. Tian, C. Liu, Q.Y. Li,et al., Appl. Catal. A : General, (2015), 506, pp. 134-142.  
 [6] T.X. Shang, X.X. Cai, X.J. Jin,et al., RSC Adv., (2015), 5, pp. 16433-16438.  
 [7] X.D. Ren, J.Z. Zhu, F.M. Du, et al., J. Phys. Chem. C, (2014), 118, pp. 22412-22418.  
 [8] Q.H.Guo, D. Zhao, S.W. Liu, et al., Electrochim. Acta, (2014), 138, pp. 318-324.  
 [9] K. Suenaga, M.P. Johansson, N. Hellgren, et al., Chem. Phys. Lett., (1999), 300, pp. 695-700.  
 [10]H. Liu, Y. Zhang, R.Y. Li, Carbon, (2010), 48, pp. 1498-1507.  
 [11]N.Gavrilov, I.A.Pašti, M.Vujkovic, Carbon, (2012), 50, pp. 3915-3927.  
 [12]Q. Liu, Z.H. Pu, C. Tang,et al., Electrochem. Commun, (2013), 36, pp. 57-61.  
 [13]F. Xu, M. Minniti, P. Barone,et al., Carbon, (2008), 46, pp. 1489-1496.  
 [14]J.Y. Yook, J. Jun, S.Kwak, et al., Appl. Surf. Sci., (2010), 256, pp. 6941-6944.  
 [15]F.Poncin-Epaillard, J.C.Brosse, T.Falher, Macromolecules, (1997), 30, pp. 4415-4420.  
 [16]V.K. Abdelkader., S. Scelfo, C. Garcia-Gallarín, et al., J. Phys. Chem. C, (2013), 117, pp. 16677-16685.  
 [17]O. Chirila, M. Totolin, G. Cazacu, et al., Ind. Eng. Chem. Res., (2013), 52, pp. 13264-13271.  
 [18]Z.H.Luo, L.H. Zhu, Y.F. Huang, et al., Synth. Met., (2013), 175, pp. 88-96.  
 [19]S.B. Wang, C.L. Xiao, Y.L. Xing, et al., J. Mater. Chem. A, (2015), 3, pp. 6742-6746.  
 [20]M.Vujković,N.Gavrilov, I.A. Pašti, et al., Carbon, (2008), 64, pp. 472-486.  
 [21]H.L. Wang, Q.L. Hao, X.J. Yang, et al., ACS Appl. Mater. Interfaces, (2010), 2, pp. 821-828.  
 [22]H. Sjöström, S. Stafström, M. Boman, et al., Phys. Rev. Lett., (1995), 75, pp. 1336-1339.  
 [23]H.Y. Liu, H.H. Song, X.H. Chen, et al., J. Power Sources, (2015), 28, pp. 5303-309.  
 [24]W. Fan, Y.E. Miao, L.S. Zhang, et al., RSC Adv., (2015), 5, pp. 31064- 31073.  
 [25]S.L. Candelaria, B.B. Garcia, D. Liu, et al., J. Mater. Chem., (2012), 22, pp. 9884-9889.  
 [26]J. Zhao, H.W. Lai, Z.Y. Lyu, Adv. Mater., (2015), 27, pp. 3541-3545.